



First Results from the Wide Angle Camera of the ROSETTA Mission

C. Barbieri¹, S. Fornasier¹, I. Bertini¹, F. Angrilli², G. A. Bianchini², S. Debei², M. De Cecco², G. Parzianello², M. Zaccariotto², V. Da Deppo³, and G. Naletto³

¹ Department of Astronomy, University of Padova – Vicolo dell'Osservatorio, 2 I-35122 Padova e-mail: barbieri@pd.astro.it

² Department of Mechanical Engineering, University of Padova – Via Venezia, 1 I-35122 Padova

³ Department of Informatics Engineering, University of Padova – Via Gradenigo, 6A I-35122 Padova

Abstract. This paper gives a brief description of the Wide Angle Camera (WAC), built by the Center of Studies and Activities for Space (CISAS) of the University of Padova for the ESA ROSETTA Mission, of data we have obtained about the new mission targets, and of the first results achieved after the launch in March 2004. The WAC is part of the OSIRIS imaging system, built under the PI-ship of Dr. U. Keller (Max-Planck-Institute for Solar System Studies) which comprises also a Narrow Angle Camera (NAC) built by the Laboratoire d'Astrophysique Spatiale (LAS) of Marseille. CISAS had also the responsibility to build the shutter and the front door mechanism for the NAC. The images show the excellent optical quality of the WAC, exceeding the specifications both in term of encircled energy (80% in one pixel over a FoV of 12×12 sq degree), limiting magnitude (fainter than the 13th in 30s exposure time through a wideband red filter) and amount of distortions.

Key words. Space vehicles: instruments – Rosetta mission – Telescopes – Techniques: photometric – Minor planets, asteroids, comets

1. Introduction

ROSETTA is the cornerstone mission of the European Space Agency (ESA) devoted to the study of the minor bodies, of fundamental importance for the comprehension of our Solar System, because they are the bodies most representative of its primordial material. The primary target is comet 67P/Churyumov-Gerasimenko, a short period comet of Jupiter's family. Secondary scientific targets are two as-

teroids, Steins and Lutetia. While the present scenario for the asteroids is fairly similar to the old one, as the new targets have many physical properties resembling the previous ones (Steins vs. Otawara, Lutetia vs. Siwa) and similar are the conditions of closest approach, the two comets 67P and 49P have important differences, as explained later on.

ROSETTA has a complex instrumentation devoted both to remote sensing and in situ investigation. The authors of the present paper were involved in the design and manufacturing

Send offprint requests to: C. Barbieri



Fig. 1. OSIRIS mounted on ROSETTA (upper edge), the WAC on the left, the NAC on the center. Part of VIRTIS are seen on the right (photo taken in ALENIA, Dec. 2001).

of the entire Wide Angle Camera (WAC) and of mechanism of the Narrow Angle Camera (NAC) which form the OSIRIS imaging system (P.I. Dr. U. Keller, Max-Planck-Institute for Solar System Studies, Germany, who also provided the Focal Plane Assembly). The camera was described in great detail by Thomas et al. (1998), and Barbieri et al. (2003), so that only some instrumental characteristics will be recalled, together with the description of the new Rosetta mission scenario and of the first WAC performances.

2. Some WAC characteristics

The WAC has the optical characteristics shown in Table 1 and Fig. 2. The primary mirror (M1) is an off-axis section of an oblate convex ellipsoid, decentered with respect to the optical axis of 43 mm and of squared shape ($53 \times 53 \text{ mm}^2$); the second one (M2) has an oblate concave ellipsoidal shape, 5 mm decentered with respect to the optical axis of the camera. M1 collects the light from the object at an angle of 20° with respect to the camera axis and sends it to M2, which focuses the light on the focal plane assembly placed 51 mm behind M1. The system stop is at the level of M2 and it is decentered by 5 mm with respect to the optical axis. The off-axis design produces two slightly different im-

Table 1. F/5.6 WAC Optical Characteristics

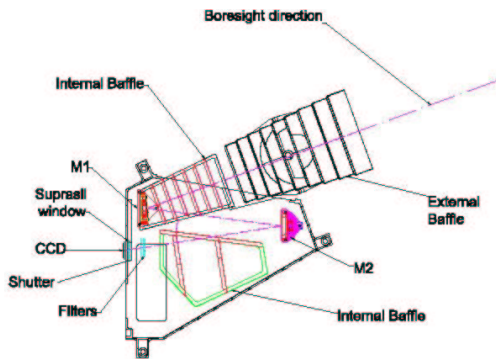
Optical concept	2 mirrors, 20° off-axis design
Axis of off-axis:	y
FoV	12.00° in x, 12.05° in y
FoV	unobstructed, unvignetted
Focal Length	132 mm (center FoV)
Image scale	1562.6 ''/mm (center FoV)
Refocusing	no necessary
Nominal F/ratio	F/5.6
photometric area	4.91 cm^2
Wavelength range	230 to 750 nm
Overall reflectivity	65%–72%
Encircled Energy	80% inside pixel
Detector	$2048 \times 2048 \text{ px}$
pixel size	$13.5 \text{ }\mu\text{m}$

age scales: the scale in x varies from 21.8 ''/px to 20.4 ''/px . Therefore the field width in x decreases from 12.4° to 11.6° , while it is constant, 12.05° , in y. The nominal photometric aperture is circular, with a radius of 1.25 cm; however, the distortion just described causes the aperture to be slightly elliptical and position dependent. Regarding the imaging properties for an object at close distance, the performance is kept essentially unchanged from infinity down to almost 500 m.

A set of 14 filters for the WAC (and 12 for the NAC) has been selected for maximum scientific return; their list is provided in Table 2. The filters were produced by Spectrogon (Sweden), under the supervision of the Uppsala Observatory. In the case of the WAC, one principal aim is to study the intensity of gas emissions and dust-scattered sunlight as functions of position and viewing angle in the vicinity of the nucleus. This is accomplished by narrow band filters centered on a set of emissions expected to be both strong and diagnostic of physical processes in the comet, and by broad band filters to study the dust as uncontaminated by gas as possible, and to provide continuum measurements close to the gas emissions in order to remove any dust contributions within the emission bandpasses. The central wavelengths span from 245 to 640 nm. For the gas emissions the bandwidth is 4 nm,

Table 2. List of WAC filters

λ (nm)	$\Delta\lambda$ (nm)	Scientific Objective
245	15	Continuum for CS
257.5	4	CS gas emission
295	10	Continuum for OH
308.5	4	OH emission
325	10	Continuum for OH-NH
335.5	4	NH gas emission
375	10	Continuum for CN
387.5	4	CN gas emission
535	60	V dust continuum
571.5	10	NH ₂ gas emission
589.1	4	Na gas emission
610	10	Continuum for O-Na
630	4	O (1D) gas emission
640	160	Broad band R

**Fig. 2.** The WAC optomechanical design.

the minimum allowed by the F/5.6 optical design. The wide R filter is aimed to detect the cometary nucleus and asteroids at large distance.

During tests of the Flight Model, the WAC UV filters showed the presence of small pinholes, that went undetected during the acceptance tests; no correcting action could be taken; therefore the WAC UV images will require careful flat fielding in flight.

The peculiar optical system, based on two aspherical mirrors in an off-axis configuration, and the primary scientific aim to study very faint gas and dust cometary features in the vicinity of the nucleus at all heliocentric

distances from 3.2 AU to the perihelion, imposed the design and construction of an innovative baffling system, in order to reach the stray-light suppression requirements both for source inside and outside the field of view. In particular, a contrast ratio of 10^{-4} inside the field of view is needed in order to detect gaseous and dusty features close to the nucleus of the comet.

Two important mechanisms are the shutter and the front door. The shutter is made up of two blades driven by two independent four-bar-mechanism devices moved by two brush-less motors. The shutter goal is to guarantee exposure times within the range 10ms - 1000s, with a minimum repetition rate of 1s for high speed imaging mode; the normal case is around 100ms for a repetition rate of 15s. The front door insures full protection from contaminants, it opens only during the scientific exposures. The internal face of the door is diffusing, insuring a flat field illumination by mean of internal lamps.

The detector is a back-illuminated, antiblooming CCD with 2048×2048 pixels, 13.3×13.5 μm each. The approximate exposure times in the 5350 Å filter (V dust continuum) can be calculated from the following equation, that gives the number of counts (C) per second:

$$C = 1080 \cdot 10^{-0.4m_v} \cdot A \cdot R^2 \cdot T \cdot \Delta\lambda \cdot Q \cdot t_e$$

where A is the photometric area (4.9 cm²), R² the overall reflectivity (0.65), T the optical transmission (0.70), $\Delta\lambda$ the bandwidth for the green filter (600 Å), Q the quantum efficiency (0.80), with a pixel full well of 1.2×10^5 e⁻, and t_e is the exposure time in seconds. Table 3 gives the V-magnitudes of stars producing about 100 counts (namely giving S/N = 10 in absence of sources of noise beyond photon statistics) in 10ms, 100ms, 1s, 10s, 30s and 60s, and the V-magnitudes of stars producing full well counts and so saturation in the same time. Regarding the sky background, if it is V=22.0 mag/arcsec², then given the pixel size of 20 × 20 arcsec², it corresponds to 19 mag/px. Even for superpixel binning 4×4 it becomes of 17.8, totally negligible.

At 3.3 AU, the apparent visual mag of the Sun

Table 3. WAC photometric performances in the V filter: limiting magnitude of stars (considering a S/N ration of about 10) and saturating stars as a function of different exposure times.

T_{exp} (s)	m_v (S/N \sim 10)	m_v (saturation)
0.01	5.0	-2.5
0.1	7.5	0.0
1	10.0	2.5
10	12.5	5.0
30	13.7	6.2
60	14.5	6.9

is 2.5 mag dimmer than at 1 AU, namely $V = -24.2$. Supposing that the comet nucleus is a disk with projected area $\sim 10 \text{ km}^2$, reflecting 4% of the Sun light, at a distance of 10^6 km and at opposition, the apparent mag of the nucleus is $-24.2 - 2.5 \log(4) - 5 \log(10^{-5}) = 4.3$. At 90° elongation, assuming that only 50% of the surface is visible and neglecting phase effects, the mag is raised to 5.8. Therefore the primary requirement of detection of comet and asteroids in 1s at 10^6 km is satisfied. The experience in flight has shown (Fig. 3 and 4) that the longest exposure times obtained till now (say 10 minutes) are limited essentially by the many cosmic rays, so that a limiting value of $m_v \sim 15$ is reachable.

3. Mission Overview

Rosetta was successfully launched on 2 March 2004. The scenario mission was completely revisited after the launch postponement due to problems with the Ariane 5 launcher (see Table 4).

3.1. Comet P/67

The main target of Rosetta has been changed from comet 46P/Wirtanen to comet 67P/Churyumov-Gerasimenko, a Jupiter family comet as the previous target, with an orbital period of 6.57 year. This comet is much larger than 67P: the nucleus has an estimated diameter of $3 \times 5 \text{ km}$, with a

Table 4. The new Rosetta mission scenario

Event	Nominal date
Launch	March 2004
First Earth gravity assist	March 2005
Mars gravity assist	March 2007
Second Earth gravity assist	November 2007
Asteroid Steins flyby	September 2008
Third Earth gravity assist	November 2009
Asteroid Lutetia flyby	July 2010
Enter hibernation	July 2011
Exit hibernation	January 2014
Rendezvous manoeuvre	May 2014
Start Global Mapping	August 2014
Lander Delivery	November 2014
Perihelion Passage	August 2015
End of Mission	December 2015

rotational period of about 12 hours. The main consequences for the change of comet are due from one side to the bigger nucleus, and on the other to the much dustier nature. The first aspect implies for the WAC a larger number of images to cover the nucleus with the same spatial resolution. Furthermore, little is known about the rotation of the nucleus itself, another important parameter to define the observational strategy. The second aspect will undoubtedly influence the choice of the filters; less gas implies the lesser utility of the UV filters, and a greater predominance of the observations in the continuum. In addition, the ambient around the comet will be dirtier.

Comet 67P was observed from Earth on six approaches to the Sun, showing that the comet is unusually active for a short period object, and has a coma and often a tail at perihelion. As 67P is larger and more active than comet 46P, the dust and gas emissions are expected to be higher in comparison to the original mission scenario. Fulle et al. (2004) identified the dust tail structure named Neck-line providing a dust mass lost rate of 300 kg s^{-1} before perihelion and 10 kg s^{-1} after perihelion. So an expected greater number of dust impacts on the spacecraft and its instrumentation are the main problem connected with the change of the target, together with the different gravitational environment determined by the larger

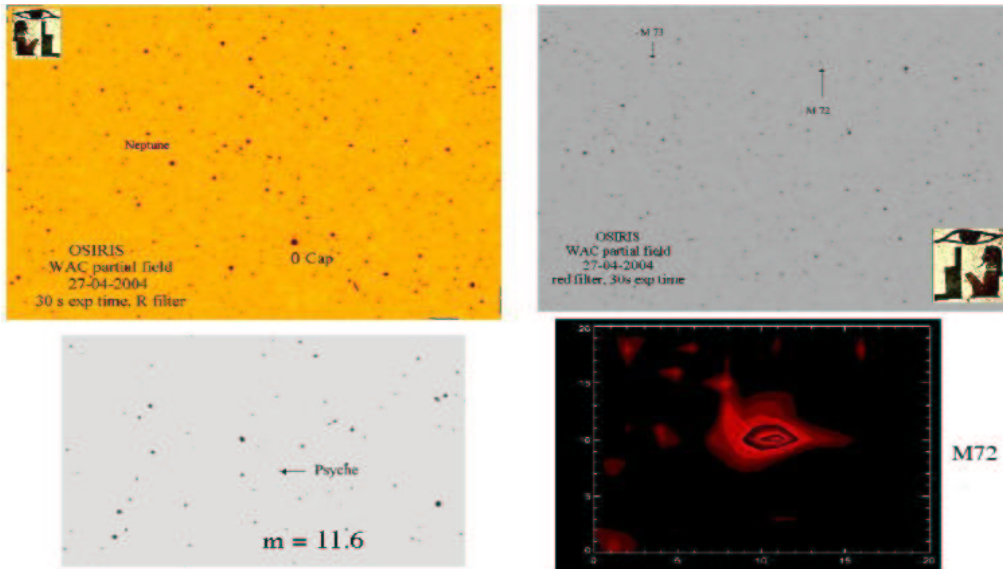


Fig. 3. This 30s exposure through the red filter covers an area of 12×12 sq deg; here the portion containing Neptune (upper left), the two globular clusters M72 and M73 (upper right), asteroid 16 Psyche (bottom left), and the isophotes plot of M72 (bottom right).

nucleus. As far as modeling of cometary dust is concerned, I. Bertini (2004) has developed a new model of structure and light scattering of individual cometary dust grains, building a code to randomly generate dust chains (dust particles) using N spheres (monomers) as constituent by means of a Particle-Cluster-Aggregation (PCA) mode. The final goal is to model the observational characteristics of the cometary dust such as the polarization and phase function curves of Sun light scattered by the cometary dust. The preliminary results show that even particles with a low fractal mass dimension can successfully reproduce qualitatively the observed scattering properties of cometary dust. Future studies will use this model to predict the luminosity of cometary dust and determine the scattering properties from a fractal microscopic point of view.

3.2. Asteroids

The fly-by with the asteroids will provide a global characterization of the objects, including determination of dynamic properties, surface morphology and composition. In particu-

lar, the main scientific goals of the WAC during the asteroid fly-by are:

- to contribute to the astrometric studies, using the rich stellar background
- to ascertain its environment, such as a possible satellite or dust coma
- to characterize the body (size, shape, pole orientation, period of rotation, density) and surface (cratering and mineralogical composition) producing a multi-band albedo map. Counts of craters will also provide an estimate of the age.
- to detect a satellite. A satellite of an asteroid is expected (from dynamical and statistical considerations) to orbit within one or very few hundreds of the parent asteroid radius.

The two asteroid (Steins and Lutetia) have fairly different properties. Steins is relatively small, with a diameter of a few kilometers, and will be visited by Rosetta on 5 September 2008 at a distance of about 1700 kilometers (TBC). This encounter will take place at a relatively low speed of about 9 km/s.

Lutetia is a much bigger object, nearly 100 km in diameter. Rosetta will pass within about 3000 km (TBC) on 10 July 2010 at a speed of 15 km/s, during Rosetta's second passage

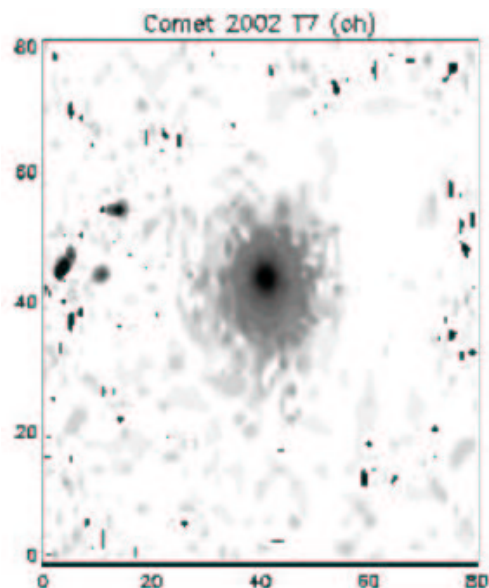


Fig. 4. A WAC 60s exposure through the OH filter of the comet 2002 T7 (image acquire on 27 April 2004).

through the asteroid belt.

However, most properties are still poorly known, so ground-based investigations have been organized by several groups to help establish the observational strategies of the spacecraft. As for the comet, we have started investigations along several lines and already published several papers (Birlan et al. 2004, Lazzarin et al. 2004, Barucci et al. 2005).

4. First images from the WAC

All OSIRIS is working well, there are excellent data obtained by the NAC, but they will be presented elsewhere. Here we show some of the first images taken after the launch (Fig. 3 and 4). Having at our disposal a huge field of view of 12×12 square deg, with a limiting magnitude fainter than the 12^{th} , we have performed a very detailed astrometric analysis of the camera, by using the USNO catalogue stars visible on the 30s red image. The camera seems to work perfectly from an optical point of view, reaching a limiting magnitude of 13th in 30s exposure time. In the first light images, planet

Neptune, asteroid 16 Psyche (mag~11.6) and M72-M73 globular clusters have been identified (Fig. 3). Already a first order analysis shows that the distortions can be calibrated to better than 0.1 pixels.

There are still some problems, mostly due to the very complex software that needs some fine tuning. A great complication is the slow telemetry which prevents a real time control of the operations, and imposes long dead times between each action. We can quote in particular some scattered light that must come from still unidentified parts of the spacecraft at particular solar positions.

Acknowledgements. Many other persons in CISAS have contributed to the success of the camera, we wish to recall G. Cremonese, M. Fulle, P.F. Brunello, S. Peron, P. Ramous. Regretfully, we have to recall the untimely departure of Paolo Zambolin, who was instrumental for the internal cabling and wiring of the camera.

References

- Barbieri, C., Fornasier, S., Verani, S., et al. 2003. MemSAIt vol. 74, 434-435.
- Birlan, M., Barucci, M. A., Vernazza, P., et al. 2004. New Astronomy, 9, 343-351
- Barucci, M. A., Fulchignoni, M., Fornasier, S., et al. 2005. A&A 430, 313-317
- Bertini I., Thomas N., & Barbieri C, COSPAR 2004
- Brunello, P. F., Peron, F., Fornasier, S., & Barbieri, C., 2000. SPIE, San Diego Aug. 2000 Da Deppo V., et al. 2001. SPIE, San Diego Aug. 2001
- Debei, S., Fornasier, S., Barbieri, C., Brunello, P., & Peron, F., 2001. SPIE AM115, San Diego Aug. 2000
- Fulle, M., Barbieri, C., Cremonese, G., et al., 2004. A&A 422, 357
- Lazzarin, M., Marchi, S., Magrin, S., & Barbieri, C., 2004. A&A 425, 25
- Naletto, G., Da Deppo, V., Pelizzo, M. G., Ragazzoni, R., & Marchetti, E. 2001. Journal of the Optical Society of America, 2001
- Thomas, N., Keller, U. H., et al. 1998. Adv. Space Res. 21(11), 1505-1515.